Hybrid mean field and alloy analogy treatment of the Hubbard model

2004 J. Phys.: Condens. Matter 16 S5221

(http://iopscience.iop.org/0953-8984/16/44/019)

INSTITUTE OF PHYSICS PUBLISHING JOURNAL OF PHYSICS: CONDENSED MATTER

J. Phys.: Condens. Matter **16** (2004) S5221–S5231 PII: S0953-8984(04)85258-5

Hybrid mean field and alloy analogy treatment of the Hubbard model

A Uldry and R J Elliott

Department of Physics, Theoretical Physics, 1 Keble Road, Oxford OX1 3NP, UK

E-mail: a.uldry1@physics.ox.ac.uk and r.elliott1@physics.ox.ac.uk

Received 23 August 2004
Published 22 October 2004
Online at stacks.iop.org/JPhysCM/16/S5221
doi:10.1088/0953-8984/16/44/019

Abstract

We propose a new treatment of the Hubbard model that is based both on the coherent-potential approximation (CPA) and the virtual-crystal approximation (VCA). It is well known that the equilibrium found using the one-particle CPA Green functions does not predict an ordered magnetic ground state, while Stoner's mean-field treatment, which is equivalent to the VCA on the Hubbard model, does so for a wide range of parameters. A hybrid treatment, the τ-CPA, is developed, in which a particle is assumed to be scattered from an array of static opposite spins for a time τ related to the inverse of the band width. The propagation is treated in the CPA over this period; thereafter the particle sees the time-averaged effect of the scatterers and hence can be treated in the VCA. This model, with suitable approximations, does predict magnetism for a modified Stoner criterion.

1. Introduction

While much progress has been made in recent years in the theoretical treatment of magnetism in the transition metals and similar materials, a complete treatment of the many aspects of these familiar but complicated systems is still lacking. The electrons retain many of their energy band properties as is reflected by their metallic behaviour, but the magnetic properties reveal that strong correlations exist between the electrons on the individual atoms, and exchange occurs between them.

The simplest treatment of metallic ferromagnets is due to Stoner [1] who assumed that the electron interaction gave rise to a molecular field which predicted ferromagnetism in a simple band model if the ratio of the interaction to the band width (or more precisely the density of states of the Fermi surface) was adequately large. But beyond the mean field the model gives no correlation between the magnetic electrons. More complex band structures also predict antiferromagnetism in some cases [2].

In recent years much more sophisticated treatments of the band structure using established methods such as those based on the spin dependent local density approximation [3–6] have been able to make much better predictions of the Fermi surface and related magnetic properties, but again a full treatment of the atomic electron correlations is lacking. Hybrid treatments such as that of Gutzwiller [7–9] which start from a mixture of correlated and uncorrelated states can give an improved treatment of the magnetic properties at the expense of some of the metallic ones.

An alternative approach to this problem has been through the study of simple band models with electron interactions, of which that due to Hubbard [10] is the simplest, which appears to contain the essence of the problem. He restricts the electron–electron interaction to occur on single atomic sites, which in the case of a single band only occurs between electrons of opposite spin because of the exclusion principle. Hubbard, in a series of papers [10, 11], pioneered different approximate treatments to this model Hamiltonian. The simplest replaces the electron–electron interaction by its average so that an electron of one spin sees a field proportional to the density of the other spin and the system has simple energy bands separated by an energy proportional to the magnetization and hence is completely equivalent to Stoner's mean field approximation. In a different vocabulary it can be regarded as a virtual crystal approximation (VCA) where the electrons move in energy bands derived from an average potential.

In order to give a better treatment of the electron–electron scattering Hubbard [11] pioneered another approximation where it was assumed that electrons of one spin were frozen on their sites and the electrons of the other spin moved through the random potential so created. He proceeded to solve this problem by determining an effective potential (which was complex and energy dependent) which took account of the average scattering from this array in an analogy with an alloy. This method has been independently used in a wide variety of alloy problems and is usually referred to as the coherent potential approximation (CPA) [12–15]. It is clear that this approximation over-estimates the electron–electron scattering and in particular causes the energy bands of each spin character to split if the interaction is large enough. As a result the tendency to ferromagnetism is under-estimated and it has been demonstrated [16, 17] that no magnetic order is predicted, except in the special case of a half filled band.

Several attempts have been made to improve on these approximate treatments, for example using a dynamical CPA [18, 19] based on the integration of this approximation into functional integral techniques. A new approach has also been developed [20] that modifies the alloy analogy so as to recover the Fermi liquid behaviour for small on-site interaction strength. This approach can be put within the larger framework of a diagrammatic treatment of the self-energy [21] that includes the dynamics of the 'frozen' spins and is exact within the local approximation. There has been a series of work where the alloy analogy [22–25] is modified in order to include a small relative shifting of the bands of the spin species based on the moment expansion for the Hubbard model. A significant theoretical development came with the dynamical mean-field theory (DMFT) [26, 27], which takes into account the quantum fluctuations in time. The DMFT is justified in the limit of infinite spatial dimensions or coordination number, where the lattice model is reduced to an Anderson impurity model and a self-consistency condition. The quantum impurity problem must then be solved, which requires sophisticated numerical techniques [28, 29] (quantum Monte Carlo simulation, exact diagonalization, numerical renormalization group. etc). Calculations for the Hubbard model have been usually restricted to temperature $T > 0$ or near half-filling [30, 31, 29]. However, the question of magnetic order at an intermediate value of the interaction strength and away from half-filling is still an open one [32].

In this work we propose a simple physical model which is intermediate between the straightforward VCA and CPA treatments. In it we assume that the random scattering centres

experienced by an electron of one type in the alloy analogy exist only for a certain time τ which is proportional to a typical hopping time between sites and hence inversely to the band width. At later times the electrons see a completely average potential reflecting the movement of the scattering centres. Thus the propagators are calculated in the CPA approximation for the short time interval τ and have to be matched to the VCA propagators which hold for longer times. Although this is a straightforward procedure in principle certain further approximations are necessary to make it tractable. The properties of the system are evaluated in this so-called τ-CPA. The single particle properties such as the density of states show, as expected, a mixture of characteristics associated with the VCA and CPA. Ferromagnetism is predicted to occur for a range of parameters which are somewhat more restrictive than those in the simple Stoner model. This paper is organized as follows: section 2 introduces the model used. The VCA and CPA methods are outlined in section 3. The τ-CPA, mixing the VCA and CPA, is constructed in section 4. Numerical results for the density of states and the magnetization using a simple cubic band are presented and discussed in section 5.

2. Model Hamiltonian

The Hubbard model is currently widely considered to be the most concise model that captures the essence of the interactions in an electronic system. It allows the hopping of the electrons from site to site to compete with the Coulomb repulsion while including the Pauli principle. We will consider the simplest case of the Hubbard model, a single-band with nearest-neighbour hopping t_{ij} and on-site repulsion:

$$H = \sum_{i,j,\sigma} t_{ij} c^{\dagger}_{i\sigma} c_{j\sigma} + U \sum_{i} c^{\dagger}_{i\uparrow} c_{i\uparrow} c^{\dagger}_{i\downarrow} c_{i\downarrow}. \tag{1}$$

$c^{\dagger}_{i\sigma}$ and $c_{i\sigma}$ are the usual creation and destruction operators for electrons in the Wannier states. The free part of the Hamiltonian H_0 is evaluated in the Bloch states $H_0 = \sum_k \epsilon_k c^{\dagger}_{k\sigma} c_{k\sigma}$ using a tight-binding approximation for the band structure ϵ_k. We will concentrate in this paper on the simple cubic band of half band width $w = 1$. As for the interaction, it is repulsive and only felt when one electron of spin σ meets another of spin $-\sigma$ at the same site. This model simulates relatively well a real material possessing narrow energy bands, like the transition metals and their alloys. We will work on a three dimensional lattice of $N = L^3$ sites, at $T = 0$. We use the framework of the canonical ensemble and fix the number N_e of electrons per atom that distribute themselves at random over the lattice sites. The Fermi statistics takes care that no site is occupied by two electrons of the same spin while the interaction favours singly occupied sites. The propagation of an electron of spin σ in the lattice can be described by the retarded Green function

$$G^{\sigma}_{ij}(t, t') = -\mathrm{i}2\pi\theta(t - t')\langle\{c_{i\sigma}(t), c^{\dagger}_{j\sigma}(t')\}_+\rangle =: \langle\langle c_{i\sigma}(t); c^{\dagger}_{j\sigma}(t')\rangle\rangle \tag{2}$$

where $\hbar$ has been set to 1. The following Fourier transform (where no particular origin is specified)

$$G^{\sigma}(E) = \frac{1}{2\pi} \int_{-\infty}^{\infty} \mathrm{d}(t - t') G^{\sigma}(t - t') \mathrm{e}^{\mathrm{i}E(t-t')} \tag{3}$$

will be used with t' set to 0. We are interested in the properties of this system averaged over all possible configurations, for which the Green function $G^{\sigma}_{k}(E)$ can be defined by

$$G^{\sigma}_{ij}(E) = \frac{1}{N} \sum_{k} G^{\sigma}_{k}(E) \mathrm{e}^{\mathrm{i}k(r_i - r_j)}. \tag{4}$$

The density of states ρ^σ is obtained from the single-particle Green function with

$$\rho^\sigma(E) = \frac{-1}{\pi} \operatorname{Im} F^\sigma(E), \tag{5}$$

where $F^\sigma(E)$ is the trace of the Green function. It can be obtained as

$$F^\sigma(E) = \frac{1}{N} \sum_k G_k^\sigma(E). \tag{6}$$

The relative proportions of the number of up-spins and down-spins must be determined self-consistently together with the chemical potential μ. Defining $N^\uparrow$ and $N^\downarrow$, respectively, as the average number of spins up and down per atom, the equilibrium conditions read

$$N^\sigma = \int_{-\infty}^{\mu} \mathrm{d}E\, \rho^\sigma(E) \tag{7}$$

with $\sigma \in \{\uparrow, \downarrow\}$.

3. VCA and CPA

The virtual-crystal approximation and the coherent-potential approximation have been both applied with various success to both the Hubbard model and the somewhat related problem of the random binary alloy $A_{1-c}B_c$. The analogy between the Hubbard model and a binary alloy was noted by Hubbard in the last paper of the series [11]. We consider a particle propagating on a lattice where each site is occupied at random either by a host atom A or an impurity atom B. The concentration of impurities is c. The model is represented by $H_{\text{alloy}} = H_o + V$, where V is a quadratic operator of the form $V = \sum_m |m\rangle \epsilon_m \langle m|$. The atomic potentials can take two values, either ϵ_A or ϵ_B, depending on whether the particle is on an A site or a B site. Setting ϵ_A to 0 and ϵ_B to U, we find that this is very similar to the Hubbard model (hence the alloy analogy), for which the spin σ propagating in the lattice interacts with energy U only on sites where a $-\sigma$ spin is present. The analogy would be exact if the spins of opposite direction could be considered as frozen in the Hubbard model.

The VCA and CPA are well established methods [15, 33] and will not be developed here. The VCA is obtained from a random phase approximation decoupling of the interaction, and is given, in the case of a binary alloy where $\langle \epsilon_m \rangle = cU$, by

$$G_k^{\text{VCA}}(E) = \frac{1}{E - \epsilon_k - cU}. \tag{8}$$

While the VCA is only a valid approximation for small perturbations V, the CPA is a particularly successful method that interpolates between the limits of strong and weak disorder and interaction. The CPA assumes the existence of an effective medium (self-energy) that is to be determined self-consistently [15, 33]. A particle moving in the effective medium sees the impurities as embedded in a uniform potential. The self-consistent condition is that the scattering generated by any single impurity is zero on average. The CPA approximation is thus given, for a binary alloy with $\epsilon_A = 0$ and $\epsilon_B = U$, by

$$G_k^{\text{CPA}}(E) = \frac{1}{E - \epsilon_k - \Sigma(E)} \qquad \text{with } \Sigma(E) = \frac{cU}{1 - [U - \Sigma(E)]F(E)}, \tag{9}$$

where $F(E)$, as in (6), is the diagonal element of the propagator. It must be determined together with $\Sigma(E)$. In the CPA Σ is an energy-dependent, k-independent complex number which accounts for the damping of the quasiparticle states by the impurities. In this form, the CPA neglects the scattering from *clusters* of atoms, though some extensions of the theory do include this effect.

The VCA treatment can be directly extended to the Hubbard model (1) if we apply the Hartree–Fock approximation to this model and effectively reducing it to a Stoner model

$$H_{\text{Stoner}} = H_0 + U \sum_i \left(N^{\uparrow} \hat{n}_{i\downarrow} + N^{\downarrow} \hat{n}_{i\uparrow} \right) \tag{10}$$

where $\hat{n}_{i\sigma} = c^{\dagger}_{i\sigma} c_{i\sigma}$ is the usual number operator. We obtain then immediately the analogy of (8) for the propagator of the up and down spins

$$G_k^{\sigma\,\text{VCA}}(E) = \frac{1}{E - \epsilon_k - N^{-\sigma} U}. \tag{11}$$

Alternatively, both the VCA and CPA can be associated with particular decoupling schemes of the equation of motion for the Green function (2) in the Hubbard model:

$$\mathrm{i}\frac{\mathrm{d}}{\mathrm{d}t} \langle\langle c_{i\sigma}(t), c^{\dagger}_{j\sigma} \rangle\rangle = 2\pi\delta(t)\delta_{ij} + \sum_l t_{il} \langle\langle c_{l\sigma}(t), c^{\dagger}_{j\sigma} \rangle\rangle + U \langle\langle \hat{n}_{i,-\sigma}(t) c_{i\sigma}(t), c^{\dagger}_{j\sigma} \rangle\rangle. \tag{12}$$

If $\hat{n}_{i,-\sigma}(t)$ is taken out of the last Green function in (12) and averaged separately, $\langle \hat{n}_{i,-\sigma}(t) \rangle \to N^{-\sigma}$, the equation of motion is decoupled and the solution is given again by (11). If, on the other hand, $\hat{n}_{i,-\sigma}(t)$ is considered at $t = 0$ and takes the value 0 or 1 at random, applying thus the alloy analogy, we retrieve the CPA result

$$G_k^{\sigma\,\text{CPA}}(E) = \frac{1}{E - \epsilon_k - \Sigma^{\sigma}(E)} \qquad \text{with } \Sigma^{\sigma}(E) = \frac{N^{-\sigma} U}{1 - [U - \Sigma^{\sigma}(E)] F^{\sigma}(E)}. \tag{13}$$

This treatment, due to Hubbard [11], has been called the 'scattering correction'. It was noted only later by Velický *et al* that the scattering correction Green function from Hubbard is equivalent to the CPA result for the alloy model.

4. The τ-CPA

It has been known for some time now that the CPA does not allow for ferromagnetic solutions [17, 16]. On the other hand, the VCA treatment of the Hubbard model leads to an artificially strong ferromagnetic phase. We propose to combine these two different approximations in order to keep the advantages of the CPA while allowing for spontaneous magnetic ordering to occur. As was seen in the previous section, the VCA and CPA take two very different views when considering the motion of a particle in the lattice. The CPA sees the scatterers as fixed at the positions given at $t = 0$, while the VCA considers the scattering events only as averaged over a time $t \to \infty$. In other words, the CPA is valid for the Hubbard model only at $t = 0$ and the VCA at $t \to \infty$. A better physical picture should emerge if the CPA treatment is applied for a short time only, when it is still reasonable to consider the scatterers as fixed. This time is typically the time needed for the particle to travel between sites. Thereafter we can assume that the VCA average provides a reasonably good treatment.

Let $G_k^{\text{VCA}}(t)$ and $G_k^{\text{CPA}}(t)$ be, respectively, the time Fourier transform of the VCA and CPA Green functions for $t \geqslant 0$. The central assumption is that up to a time $\tau > 0$ and $\tau \approx 1/w$ the system is described by the CPA Green function, whereas beyond τ it is described by the VCA Green function. A new function $g_k^{\tau\,\text{CPA}}(t)$ is defined as

$$g_k^{\tau\,\text{CPA}}(t) = -\mathrm{i}2\pi\theta(\tau - t) G_k^{\text{CPA}}(t) - \alpha \mathrm{i}2\pi\theta(t - \tau) G_k^{\text{VCA}}(t). \tag{14}$$

At $t = 0$, $g_k^{\tau\,\text{CPA}}$ is equal to the CPA Green function and is thus properly normalized. A factor α, the 'matching factor', has been introduced to ensure the continuity of the wavefunction at time τ.

The retarded Green functions for the VCA and CPA are given, respectively, by G_k^{VCA} (8) and G_k^{CPA} (9). The Fourier transform reads:

$$G_k(t) = \int_{-\infty}^{\infty} \mathrm{d}E\, \mathrm{e}^{-\mathrm{i}Et} G_k(E). \tag{15}$$

It is straightforward to obtain $G_k^{\mathrm{VCA}}(t)$ by contour integration in the lower half of the complex plane. There is one pole at $z_0 = \epsilon_k + cU - \mathrm{i}\delta$, so that

$$G_k^{\mathrm{VCA}}(t) = -\mathrm{i}2\pi\theta(t)\mathrm{e}^{-\mathrm{i}(\epsilon_k + cU)t}. \tag{16}$$

It is more difficult to do a similar calculation for the CPA. The problem lies in the nature of the CPA poles. It has been noted by Velický *et al* [33] that the two complex CPA poles cannot in all generality be interpreted as quasiparticle energy, and their analytical continuations cannot be simply used to obtain the correct inverse Fourier transform. We assume instead, by similarity with the VCA:

$$G_k^{\mathrm{CPA}}(t) = -\mathrm{i}2\pi\theta(t)\mathrm{e}^{-\mathrm{i}(\epsilon_k + \Sigma)t}. \tag{17}$$

At this stage the fact that Σ is an energy-dependent quantity is ignored, and Σ is treated as a fixed quantity rather than a function. By doing so, Fourier-transforming (17) gives the correct result (9). The substitution $\Sigma \to \Sigma(E)$ must be made thereafter. The whole $g_k^{\tau\mathrm{CPA}}(t)$ is still normalized at $t = 0$, but because of the dependence of Σ on the energy, this does not guarantee the normalization of $g_k^{\tau\mathrm{CPA}}(E)$. The normalization will have to be corrected numerically.

The integrals for the Fourier transform on the partial intervals give, without taking into account the matching factor α,

$$\mathcal{G}_k^{\mathrm{VCA}}(E) = \frac{1}{2\pi}\int_0^{\tau} \mathrm{d}t\, \mathrm{e}^{\mathrm{i}Et} G_k^{\mathrm{VCA}}(t) = \frac{\mathrm{e}^{\mathrm{i}(E-\epsilon_k-cU)\tau}}{E-\epsilon_k-cU} \tag{18}$$

$$\mathcal{G}_k^{\mathrm{CPA}}(E) = \frac{1}{2\pi}\int_{\tau}^{\infty} \mathrm{d}t\, \mathrm{e}^{\mathrm{i}Et} G_k^{\mathrm{CPA}}(t) = \frac{1-\mathrm{e}^{\mathrm{i}(E-\epsilon_k-\Sigma)\tau}}{E-\epsilon_k-\Sigma}. \tag{19}$$

The $\mathcal{G}_k^{\mathrm{VCA}}(E)$ and $\mathcal{G}_k^{\mathrm{CPA}}(E)$ are the standard VCA and CPA Green functions, weighted by a complex τ-dependent quantity.

The factor α that forces the CPA and VCA Green functions to match at $t = \tau$ is found to be

$$\alpha = \mathrm{e}^{-\mathrm{i}(\Sigma - cU)\tau}. \tag{20}$$

This value for α can be reintroduced into (14). The result for $g_k^{\tau\mathrm{CPA}}(E)$ is then obtained from the Fourier transform of (14):

$$g_k^{\tau\mathrm{CPA}}(E) = \frac{1}{2\pi}\int_0^{\infty} \mathrm{d}t\, G_k^{\tau\mathrm{CPA}}(t)\mathrm{e}^{\mathrm{i}Et}\frac{1-\mathrm{e}^{\mathrm{i}(E-\epsilon_k-\Sigma)\tau}}{E-\epsilon_k-\Sigma} + \frac{\mathrm{e}^{\mathrm{i}(E-\epsilon_k-\Sigma)\tau}}{E-\epsilon_k-cU} \tag{21}$$

Σ is now read as $\Sigma(E)$, as calculated by the pure CPA equation (9). The expression (17) now reproduces exactly the CPA behaviour in the limit $\tau \to \infty$. The VCA approximation is retrieved in the limit $\tau \to 0$.

We recall that the normalization of the Green function has been lost by choosing to ignore the energy dependence of Σ. It is therefore necessary to calculate numerically for each k the factor β_k, so that $\beta_k^{-1} g_k^{\tau\mathrm{CPA}}(E)$ is normalized.

The result (21) is, however, not giving a physical density of states: $\rho(E)$ changes sign along the E axis. By stopping the Green function at a time τ we have in fact introduced a non-physical oscillatory term coming from the factor weighing VCA and CPA

$$\mathrm{e}^{\mathrm{i}(\omega-\epsilon_k-\Sigma)\tau} = \mathrm{e}^{\mathrm{i}(\omega-\epsilon_k-\mathrm{Re}\,\Sigma)\tau}\mathrm{e}^{\mathrm{Im}\,\Sigma\tau}. \tag{22}$$

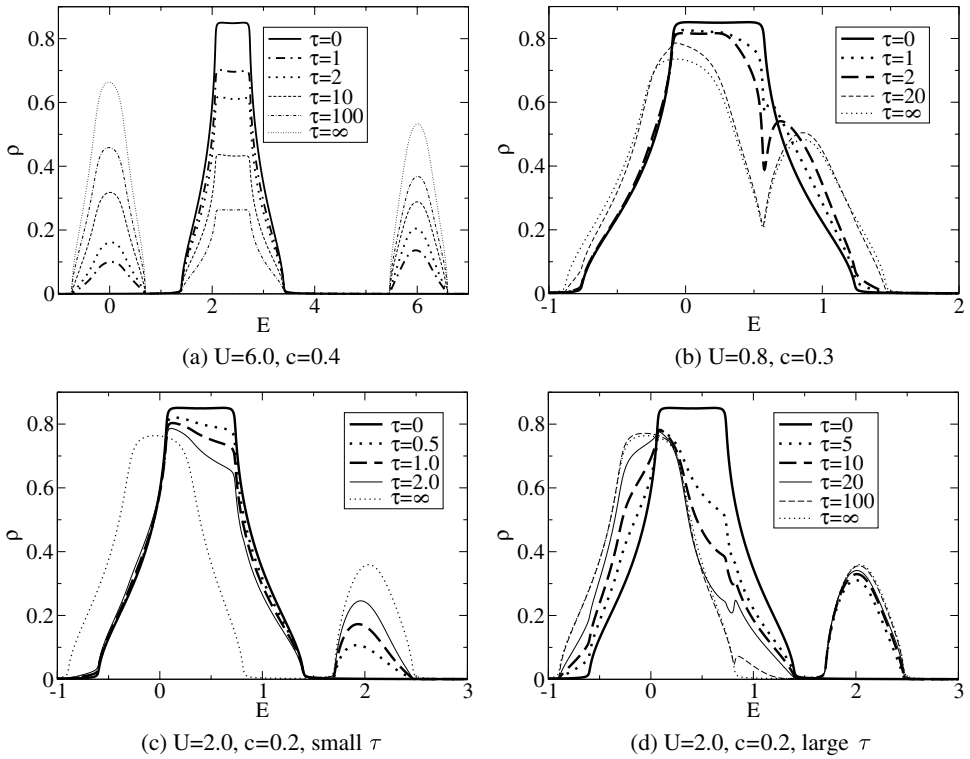

(a) U=6.0, c=0.4 (b) U=0.8, c=0.3

(c) U=2.0, c=0.2, small τ (d) U=2.0, c=0.2, large τ

Figure 1. DOS ρ for the τ-CPA using a simple cubic band with $w = 1$, for various values of the concentration and interaction.

The oscillatory term destroys the analytical properties of the CPA and VCA. The imaginary part of $N^{-1}\sum_k -\pi^{-1} g_k^{\tau\mathrm{CPA}}(E + \mathrm{i}\delta)$ does not give the physical density of states, as the branch cut no longer runs along the x-axis. It is thus necessary to smooth out the Green function by putting the oscillatory term to unity. We obtain finally

$$G_k^{\tau\mathrm{CPA}}(E) = \frac{1}{\beta_k}\left(\frac{1 - \mathrm{e}^{\mathrm{Im}\,\Sigma(E)\tau}}{E - \epsilon_k - \Sigma(E)} + \frac{\mathrm{e}^{\mathrm{Im}\,\Sigma(E)\tau}}{E - \epsilon_k - cU}\right). \tag{23}$$

This function now possesses all the properties required. It interpolates between a pure VCA Green function at $\tau \to 0$ and the CPA Green function at $\tau \to \infty$. We observe that (23) is decomposed into a CPA and VCA contribution weighted by a real τ-dependent factor. Although τ is not strictly determined by the problem, a reasonable value for it is given on physical grounds by the band width.

5. Numerical results and discussion

In this section, the τ-CPA Green function (23) is used to obtain the density of states for both species of spins in the Hubbard model. Various values of the impurity concentration c (c corresponds to either $N^{\uparrow}$ or $N^{\downarrow}$), of the interaction U and of τ are considered. Calculations are made for a simple cubic band with $w = 1$. Another one-particle property is then evaluated, the magnetization m versus the interaction strength U, for a various range of parameters.

The density of states is obtained from the Green function (23) using (5) and (6). Figure 1(a) shows the density of states obtained for a strong disorder and interaction strength, $U = 6.0$

and $c = 0.4$. τ is varied from 0 (pure VCA) to $\tau \to \infty$ (pure CPA). At $\tau = 0$ the spectrum exhibits the single VCA band, centred at $E = cU$. As τ increases, the two CPA sub-bands appear, at $E = 0$ for the main band and $E = U$ for the impurity band. Weight is transferred from the VCA band to both the CPA sub-bands, affecting all the three sub-band heights, but not their general shape. At $\tau \to \infty$ the VCA band has disappeared and only the two CPA sub-bands survive, with their original, pure CPA respective weight. In this graph the τ-CPA merges with the pure CPA at $\tau \approx 600$.

More dramatic effects on the band shapes occur at smaller U, when the bands mix. Figure 1(b), for $U = 0.8$ and $c = 0.3$, depicts a case for which U and c are sufficiently small so that the pure CPA sub-bands are not split. As τ increases, the height of the VCA band decreases while that of the main CPA sub-band increases. The general picture produced in that case is that for $\tau > 0$, the degenerate states near the centre of the VCA band start to scatter, while the edges of the band are still untouched. For larger τ, the states continue to diffuse to the impurity band from the centre to the right edge. At the same time, states of lower energy are being occupied, re-centring the created sub-band around 0. Cases at intermediate U are not so smooth, as can be seen in figures 1(c) and (d), where $U = 2.0$ and $c = 0.2$. In this figure the density of states of the τ-CPA becomes equal to that of the CPA for $\tau \approx 250$. The mixing of the bands produces irregular features as the diminishing VCA meets the increasing main CPA band at larger τ, figure 1(d). This is due to the fact that a large imaginary part at an energy E favours the CPA behaviour compared to that of the VCA. The CPA self-energy has an imaginary part only within the CPA bands. When the VCA band is centred within the main CPA band but is sufficiently distinct from it, its flat top can be sharpened if close to the top of the CPA band, producing the small peaks in figure 1(d). Such drops in the VCA part of the density of states also occur for the parameters of figure 1(b). However under these conditions the VCA band is only slightly shifted from the CPA band, and the sharp peaks are compensated by the CPA part.

The τ-CPA offers a treatment that leads to density of states that interpolate between the pure VCA and the pure CPA. As will be shown in this section, the method also interpolates the value of the magnetization versus the interaction strength U between the VCA ground state (ordered ground state for sufficiently large U) and the CPA ground state (no ordered ground state at any U). We only consider in this paper the competition between paramagnetic and ferromagnetic ground states.

The equilibrium conditions for a certain U and a given, fixed number of spins N_e, are found by iteration from equations (5)–(7) and (23). The paramagnetic solution $N^\uparrow = N^\downarrow$ is always a solution. If another solution is found, its stability must be tested against the paramagnetic case by measuring the total energy of both solutions. The total energy E of the system is found by summing up the separate energies of the two spins [16, 22]

$$E = \tfrac{1}{2} \int_{-\infty}^{\mu} \mathrm{d}\omega \sum_{k,\sigma} (\omega + \epsilon_k) A_\sigma(k, \omega) \tag{24}$$

where $A_\sigma(k, \omega)$ is the spectral density defined by $A_\sigma(k, \omega) = -\pi^{-1} \operatorname{Im} G_k^\sigma(\omega)$. Diagrams of magnetization $m = N^\downarrow - N^\uparrow$ versus interaction strength U can be calculated for any value of N_e. In figure 2 the magnetization is depicted for a range of values of U. τ is fixed to 1 and the curves calculated for various filling. The first observation is that at no value of N_e ($N_e < 1$) is there saturated ferromagnetism. This is due to the residual CPA part around $E = 0$ that is never totally empty. We can also see that at $N_e \approx 0.4$ the maximum of the magnetization is not at large U: m increases at around $U \approx 8$ to reach its peak at $U \approx 2$. Keeping the filling constant ($N_e = 0.4$ and 0.7, respectively), while varying τ give the plots of figures 3(a) and (b). The magnetization is interpolated between its VCA value at $\tau = 0$ and the CPA value at $\tau = \infty$.

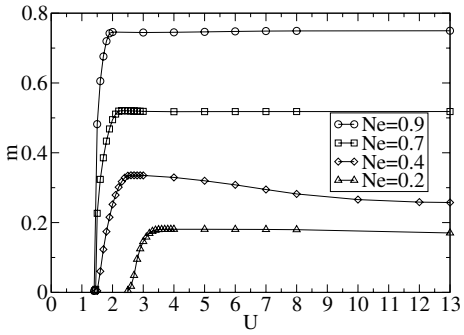

Figure 2. Magnetization m versus interaction U for the τCPA at $\tau = 1$ and various filling N_e.

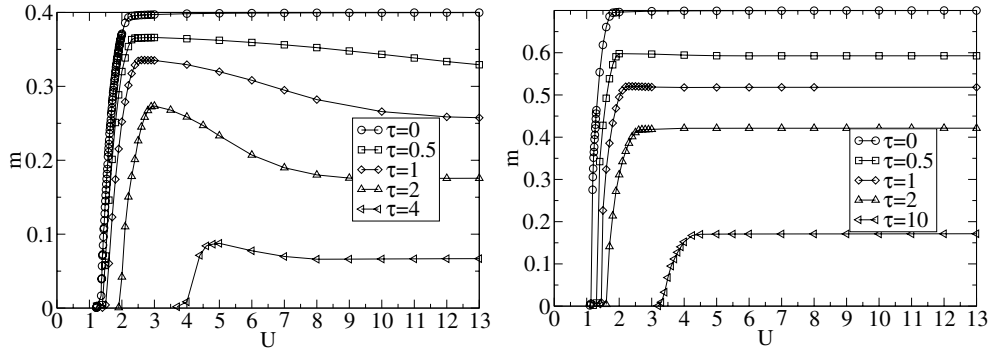

(a) $N_e = 0.4$ (b) $N_e = 0.7$

Figure 3. Magnetization m versus interaction U for the τCPA at various τ but at fixed fillings.

At $\tau = 0$ and for the fillings considered, the system is fully polarized at large enough U. The magnetization has already dropped to zero for any U at $\tau = 10$ for $N_e = 0.4$, and at $\tau = 50$ for $N_e = 0.7$. The increase in m before the drop in magnetization is particularly acute for $N_e = 0.4$ and $\tau = 2.0$, and is an artifact of the model caused by the position of the chemical potential in the VCA and CPA sub-bands. Figure 4 shows the respective positions of the CPA and the VCA sub-bands and the chemical potential for $N_e = 0.4$, compared with $N_e = 0.7$ at $\tau = 2.0$. At large U, the density of states of the up-spins (the minority spins) exhibits three well separated sub-bands for both fillings $N_e = 0.4$ and 0.7. The lower CPA sub-band is completely full. As U decreases, the VCA band gets closer to the lower CPA sub-band, in both the up-and down-spin DOS. At first, only the down-spin bands are affected, meaning that the chemical potential travels down the energy scale while the proportion of up-spins and down-spins remains more or less constant. This is the situation illustrated in the two uppermost plots of figure 4. When U is further decreased, the chemical potential will eventually reach the edge of the CPA lower sub-band. At a filling of $N_e = 0.4$, this is happening at a fairly large U, $U \approx 8.0$, so that the VCA band is still well separated (plot in the middle of the left-hand side, figure 4). $N\uparrow$ will thus decrease until the VCA band merges with the CPA band (bottom plot on the left, figure 4). For a higher filling, the two sub-bands merge before or at the same time as the chemical potential gets into the CPA band. The density of states at the chemical potential thus rapidly increases for the up-spins, and the magnetization decreases accordingly as the up-spin band matches the down-spin band.

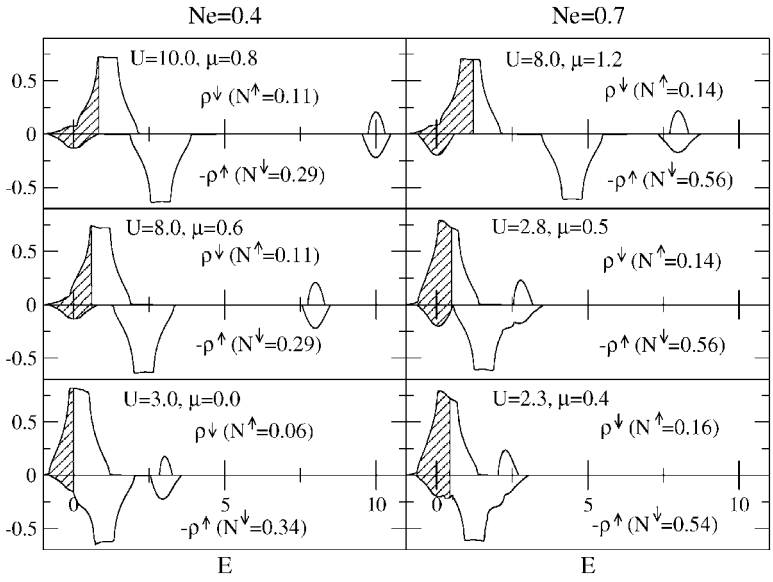

Figure 4. Density of states for both the up and down particles in the τCPA with $\tau = 2.0$. On the left the concentration is kept at $N_e = 0.4$ for $U = 10.0$, 8.0 and 3.0. On the right $N_e = 0.7$ and $U = 8.0$, 2.8 and 2.3. Occupied states are marked by the hatched area.

The increase in m at intermediate U, though also occurring at other small fillings, becomes dramatic around $N_e \approx 0.4$ and $\tau \approx 2.0$. It is at this order of magnitude of τ that the system, at $N_e \approx 0.4$, exhibits a balanced CPA-VCA behaviour. At much smaller τ, the relative weight of the CPA band becomes very small compared to the VCA part. The chemical potential falls within the CPA sub-band of the up-spin over a large range of U before the up-spin VCA band reaches it. At large τ the system becomes more CPA in character with a small VCA part responsible for the low magnetization.

The central (VCA) peak in our treatment, though bearing some similarities with the DMFT resonance peak, has a rather different origin. In the DMFT, the N-body problem is mapped into a single-impurity model which must be solved. This gives rise to a Kondo effect which builds up the Fermi-liquid quasiparticles and produces a resonance peak at the Fermi energy for small and intermediate values of U. In our case, the VCA peak is present at all strength of U, with a weight controlled by the value of τ.

6. Conclusion

A new treatment of the Hubbard model is proposed that combines the physical pictures and respective advantages of the CPA and the VCA. It is based on the fact that the CPA on the Hubbard model considers the scatterers as fixed at their positions at $t = 0$, whereas the VCA performs a time-average of the system. The one-particle Green function in the so-called τ-CPA is built from the one-particle time Green functions of the CPA and VCA. The CPA Green function is applied up to a time τ, thereafter the VCA Green function, multiplied by a factor for continuity, is used. This time τ is taken to be of the order of magnitude of the time the spins travel between sites, that is τ has the value of the inverse of the band width. The resulting Green function, which must be first smoothed out and normalized, interpolates between the VCA propagator at $\tau = 0$ and the CPA propagator at $\tau = \infty$. The density of states at finite τ

exhibits both the CPA sub-bands (or one CPA band, if U is small) and a VCA band. The bands are weighted according to the value of τ. The CPA sub-bands are fixed at their positions at $E = 0$ and U, while the VCA band, centred at $E = cU$, moves along with the concentration c. Equilibrium conditions with a polarized ground state are therefore found that are more stringent than the Stoner criterion for finite τ.

Artifacts of the τ-CPA mixture include some non-regular features in the density of states for a range of parameters (intermediate U and concentration), and peculiar behaviour of the m versus U curves at large τ and small concentration. The τ-CPA is however a successful method for the Hubbard model that is based on the better physical picture given by the combination of the CPA and VCA. It allows the treatment of the scattering by the CPA while also predicting ordered ground state for large enough U. In a next publication [34], it will be shown that the τ-CPA can also be used to calculate two-particle Green functions. In particular the dynamical susceptibility in the Hubbard model can be evaluated using this method.

Acknowledgments

AU acknowledges the support of the Swiss National Science Foundation, the Berrow scholarship trust of Lincoln College and the ORS award scheme.

References

[1] Stoner E C 1938 *Proc. R. Soc.* A **165** 372
[2] Penn D R 1966 *Phys. Rev.* **142** 350
[3] Terakura K, Oguchi T, Williams A R and Kübler J 1984 *Phys. Rev.* B **30** 4734
[4] Svane A and Gunnarsson O 1990 *Phys. Rev. Lett.* **65** 1148
[5] Anisimov V I, Aryasetiawan F and Lichtenstein A 1997 *J. Phys.: Condens. Matter* **9** 767
[6] Lichtenstein A I and Katsnelson M I 1998 *Phys. Rev.* B **57** 6884
[7] Gutzwiller M C 1963 *Phys. Rev. Lett.* **10** 159
[8] Gebhard F 1990 *Phys. Rev.* B **41** 9452
[9] Bünemann J B, Weber W and Gebhard F 1998 *Phys. Rev.* B **57** 6896
[10] Hubbard J 1963 *Proc. R. Soc.* A **276** 38
[11] Hubbard J 1964 *Proc. R. Soc.* A **281** 401
[12] Lax M 1951 *Rev. Mod. Phys.* **23** 287
[13] Taylor D W 1967 *Phys. Rev.* **156** 1017
[14] Soven P 1967 *Phys. Rev.* **156** 809
[15] Elliott R J, Krumhans J A and Leath P L 1974 *Rev. Mod. Phys.* **46** 465
[16] Schneider J and Drchal V 1975 *Phys. Status Solidi* b **68** 207
[17] Harris A and Lange V 1967 *Phys. Rev.* **157** 157
[18] Kakehashi Y 1992 *Phys. Rev.* B **45** 7196
[19] Kakehashi Y 2002 *Phys. Rev.* B **65** 184420
[20] Edwards D M and Hertz J A 1990 *Physica* B **163** 527
[21] Edwards D M 1993 *J. Phys.: Condens. Matter* **5** 161
[22] Nolting W and Borgiel W 1989 *Phys. Rev.* B **39** 6962
[23] Hermann T and Nolting W 1996 *Phys. Rev.* B **53** 10579
[24] Potthoff M, Hermann T and Nolting W 1998 *Eur. Phys. J.* B **4** 485
[25] Borgiel W, Hermann T, Nolting W and Kosimow R 2001 *Acta Phys. Pol.* B **32** 383
[26] Metzner W and Vollhardt D 1989 *Phys. Rev. Lett.* **62** 324
[27] Müller-Hartmann E 1989 *Z. Phys.* B **76** 211
[28] Georges A, Kotliar G, Krauth W and Rozenberg M J 1996 *Rev. Mod. Phys.* **68** 13
[29] Bulla R, Hewson A C and Pruschke Th 1998 *J. Phys.: Condens. Matter* **10** 8365
[30] Jarrell M 1992 *Phys. Rev. Lett.* **69** 168
[31] Obermeier Th, Pruschke Th and Keller J 1997 *Phys. Rev.* B **56** R8479
[32] Zitzler R, Pruschke Th and Bulla R 2002 *Eur. Phys. J.* B **27** 473
[33] Velický B, Kirkpatrick S and Ehrenreich H 1968 *Phys. Rev.* **175** 747
[34] Uldry A and Elliott R J 2003 *Preprint* cond-mat/0304083